Unexpected Rearrangement Reaction of Lewis Base Stabilized Group 13/15 Compounds with Group 13 Trialkyls

Florian Thomas, Stephan Schulz,* Heidi Mansikkamäki, and Martin Nieger

Institut für Anorganische Chemie, Universität Bonn, Gerhard-Domagk-Strasse 1, D-53121 Bonn, Germany

Received May 9, 2003

Reactions of the monomeric, Lewis base stabilized phosphinoalane dmap−$Al(Me)_2P(SiMe_3)_2$ with MMe_3 (M = Al, Ga, In) yielded the novel compounds dmap−$Al(Me)_2P(SiMe_3)_2$−MMe_3 (M = Al (**1**), Ga (**2**), In (**3**)). **1**−**3** are stable in their pure form, whereas they easily undergo rearrangement reactions in solution with Al−P bond breakage and methyl group transfer, resulting in the formation of dmap−$AlMe_3$ and the corresponding heterocycle $[Me_2MP(SiMe_3)_2]_x$ (M = Al, Ga, In), as was demonstrated by detailed temperature-dependent heteronuclear NMR studies. MMe_3 adducts of the stibinoalane dmap−$Al(Me)_2Sb(SiMe_3)_2$ are even more susceptible to this rearrangement reaction and cannot be isolated, whereas reactions with sterically more demanding M(*t*-Bu)$_3$ (M = Al, Ga) yielded the corresponding stable adducts dmap−$Al(Me)_2Sb(SiMe_3)_2$−M(*t*-Bu)$_3$ (M = Al (**4**), Ga (**5**)). **1**−**5** contain both regular σ-bonds and dative bonds between group 13 and group 15 elements to a single pnicogen center. **2**, **4**, and **5** were characterized by single-crystal X-ray diffraction.

Introduction

Monomeric and heterocyclic group 13/15 compounds of the type $[R_2M-ER'_2]_x$ (x = 1−3; M = Al, Ga, In; E = N, P, As, Sb (Bi)) have been synthesized and structurally characterized in large numbers.[1] Heterocycles, which are simple *head-to-tail adducts*, form due to the strong tendency of the amphoteric $[R_2M-ER'_2]$ main-group-element fragment to simultaneously react as a Lewis acid (group 13 element M) and a Lewis base (group 15 element E). The affinity of both central elements toward a tetrahedral coordination geometry (coordination number 4 instead of 3) restricts monomeric compounds $R_2M-ER'_2$ to the use of very bulky substituents (kinetic stabilization).[2] However, the reactivity of such sterically encumbered monomers is quite low, which severely limits their utility to serve as reagents in preparative organometallic chemistry. In contrast, electronically stabilized monomers of the type dmap−$M(R)_2E(SiMe_3)_2$ (R = Me, Et; M = Al, Ga; E = P, As, Sb, Bi),[3] whose general synthesis by cleavage of the corresponding heterocycles with 4-(dimethylamino)pyridine (DMAP) was recently introduced by our group,[4] are more reactive. Their ability to serve as main-group-element ligands in coordination chemistry was demonstrated in several reactions with different transition-metal complexes.[5] Consequently, we became interested in exploring their reactivity toward main-group-element compounds. We focused our interest on reactions with group 13−trialkyls MR_3 in order to investigate group 13/15 compounds containing both "regular" M−E σ and M−E dative bonds to a single pnicogen center. Only N-bridged compounds of this particular type, most of them containing a heterocyclic iminoborane moiety, have been structurally characterized to date.[6] Such reactions would create the first general pathway for the synthesis of group 13/15 compounds containing *two different* group 13 elements bridged by one group 15 element, which are of interest due to their potential application to serve as *single-source precursors* for the synthesis of ternary group 13/15 materials.[7]

Herein we report on our initial studies concerning the reactions of monomeric, base-stabilized phosphino- and stibinoalanes dmap−$Al(Me)_2E(SiMe_3)_2$ (E = P, Sb) with group 13 trialkyls MMe_3 (M = Al, Ga, In) and M(*t*-Bu)$_3$ (M = Al, Ga) and describe the solid-state structures of three novel compounds of the type dmap−$Al(Me)_2E(SiMe_3)_2$−MR_3.

Results and Discussion

Equimolar amounts of the trialkyls Me_3M (M = Al, Ga, In) were added to solutions of dmap−$Al(Me)_2P$-

* To whom correspondence should be addressed. Phone: +49 (0)228 73-5326. Fax: +49 (0)228 73-5327. E-mail: sschulz@uni-bonn.de.

(1) (a) Cowley, A. H.; Jones, R. A. *Angew. Chem., Int. Ed. Engl.* **1989**, *28*, 1208. (b) Wells, R. L. *Coord. Chem. Rev.* **1992**, *112*, 237. (c) Carmalt, C. J. *Coord. Chem. Rev.* **2001**, *223*, 217. (d) Schulz, S. *Coord. Chem. Rev.* **2001**, *215*, 1.

(2) For a comprehensive review see: Power, P. P. *Chem. Rev.* **1999**, *99*, 3463.

(3) (a) Schulz, S.; Nieger, M. *Organometallics* **2000**, *19*, 2640. (b) Kuczkowski, A.; Thomas, F.; Schulz, S.; Nieger, M. *Organometallics* **2000**, *19*, 5758. (c) Thomas, F.; Schulz, S.; Nieger, M. *Eur. J. Inorg. Chem.* **2001**, 161.

(4) Prior to our studies, some Lewis base-stabilized monomers were synthesized (for references see ref 3c). However, no prediction whether the monomer or the heterocycle would be formed was possible.

(5) (a) Thomas, F.; Schulz, S.; Nieger, M. *Organometallics* **2001**, *20*, 2405. (b) Thomas, F.; Schulz, S.; Nieger, M.; Nättinen, K. *Chem. Eur. J.* **2002**, *8*, 1915.

(6) (a) Anton, K.; Fusstetter, H.; Nöth, H. *Chem. Ber.* **1981**, *114*, 2723. (b) Anton, K.; Nöth, H. *Chem. Ber.* **1982**, *115*, 2668. (c) Anton, K.; Euringer, C.; Nöth, H. *Chem. Ber.* **1984**, *117*, 1222. (d) Anton, K.; Nöth, H.; Pommerening, H. *Chem. Ber.* **1984**, *117*, 2495. (e) Hellmann, K. W.; Bergner, A.; Gade, L. H.; Scowen, I. J.; McPartlin, M. *J. Organomet. Chem.* **1999**, *573*, 156. (f) Robinson, G. H.; Pennington, W. T.; Lee, B.; Self, M.; Hrncir, D. C. *Inorg. Chem.* **1991**, *30*, 809.

10.1021/om0303451 CCC: $25.00
Publication on Web 07/22/2003

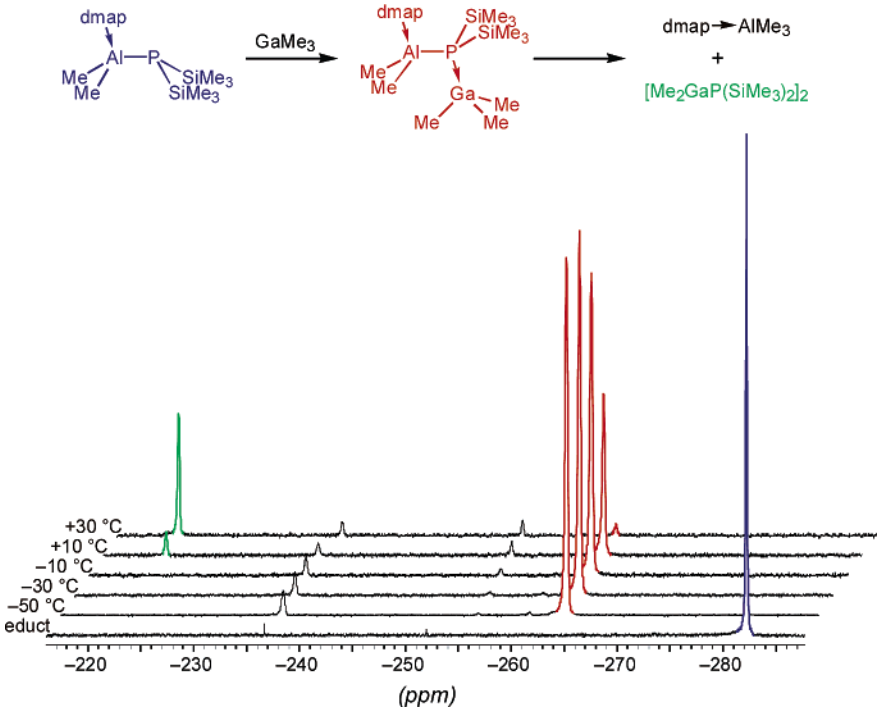

Figure 1. Temperature-dependent ^{31}P NMR spectra of **2** in toluene-d_8 between −50 and +30 °C.

$$\text{dmap}-\text{Al(Me)}_2\text{P(SiMe}_3)_2 + \text{MMe}_3 \xrightarrow{-30\ ^\circ\text{C}} \text{dmap}-\text{Al(Me)}_2\text{P(SiMe}_3)_2-\text{MMe}_3 \xrightarrow{\text{room temp}}$$

M = Al (**1**), Ga (**2**), In (**3**)

$$\text{dmap}-\text{AlMe}_3 + {}^1/_2[\text{Me}_2\text{MP(SiMe}_3)_2]_2 \quad (1)$$

$(SiMe_3)_2$ in pentane/Et_2O at −30 °C (eq 1). Within 5 min colorless solids precipitated that were isolated by filtration. NMR spectra (^1H, $^{13}C\{^1H\}$, $^{31}P\{^1H\}$) obtained from solutions of as-prepared solids in C_6D_6 at ambient temperature surprisingly displayed not only signals of the expected adducts dmap−$Al(Me)_2P(SiMe_3)_2$−MMe_3 (M = Al (**1**), Ga (**2**), In (**3**)) but also signals due to the simple Lewis base adduct dmap−$AlMe_3$ and heterocycles $[Me_2MP(SiMe_3)_2]_2$ (M = Al, Ga, In) as major components.[8] Mass spectra of **1**−**3** did not show the molecular ion peaks. Only smaller fragments such as MMe_2^+ (M = Al (*m*/*z* 57), Ga (*m*/*z* 99), In (*m*/*z* 145)), $dmap^+$ (*m*/*z* 122), dmap−$AlMe_2^+$ (*m*/*z* 179), and $P(SiMe_3)_3^+$ (*m*/*z* 250) could be detected, due to excessive fragmentation under these conditions.

Obviously, **1**−**3** are not stable at ambient temperature and undergo consecutive reactions under these conditions. In the case of dmap−$Al(Me)_2P(SiMe_3)_2$−$AlMe_3$ (**1**), a simple Lewis base transfer reaction may explain the formation of dmap−$AlMe_3$ and $[Me_2AlP(SiMe_3)_2]_2$. Here the Lewis base dmap would rather coordinate to the more Lewis acidic and sterically less crowding $AlMe_3$ than to $Al(Me)_2P(SiMe_3)_2$. However, this simple model cannot account for the products obtained from the reactions with $GaMe_3$ and $InMe_3$. At least the last two cases require a more complex reaction mechanism to explain the observed exchange of the group 13 element in the group 13/15 fragment.

Scheme 1

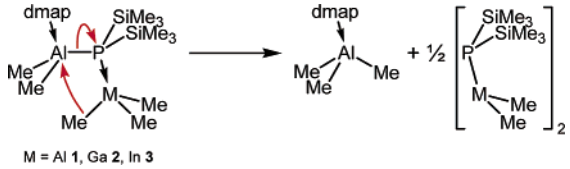

To elucidate this rearrangement reaction, we performed temperature-dependent NMR experiments of **2**, which was generated in situ by reaction of dmap−Me_2-$AlP(SiMe_3)_2$ with $GaMe_3$ at −50 °C (see Figure 1 for ^{31}P NMR spectra between −50 and +30 °C). Obviously the coordination of the Lewis acid $GaMe_3$ to the phosphinoalane takes place even at very low temperatures. From −50 to −10 °C only signals due to the adduct **2** (−262 ppm) are prevalent, and even at −50 °C no starting phosphinoalane (−282 ppm) is detected. At temperatures above −10 °C an additional signal due to the formation of the heterocycle $[Me_2GaP(SiMe_3)_2]_2$ (−219 ppm) begins to appear in the spectra, which increases upon heating to ambient temperature. The heterocycle is most likely formed by a methyl group transfer from Al to M under simultaneous Al−P bond cleavage, as shown in Scheme 1. This reaction pathway results in a metal exchange in the group 13/15 fragment (>Al−P< → >M−P<). The accuracy of this model is further supported by the reaction of the phosphinoalane with $GaEt_3$, which leads under transfer of one ethyl

(7) Wells et al. reported on group 13/15 heterocycles containing two different group 15 elements. Whether these are true ternary compounds in the solid state or simple 1:1 cocrystallized mixtures of the starting heterocycles could not be proven beyond doubt, but their thermal decomposition yielded ternary materials. Comparable results were found in our group for analogous systems containing two different group 13 elements (see also ref 1d).

(8) The signals were identified by comparison to NMR spectra of pure samples of the heterocycles $[Me_2ME(SiMe_3)_2]_x$ (see: Thomas, F.; Schulz, S.; Nieger, M. *Z. Allg. Anorg. Chem.* **2002**, *628*, 235 and references cited therein) and adducts dmap−$AlMe_3$. dmap−$AlMe_3$ was previously unknown and will be discussed elsewhere in more detail (Thomas, F.; Bauer, T.; Schulz, S.; Nieger, M. *Z. Anorg. Allg. Chem.*, in press.)

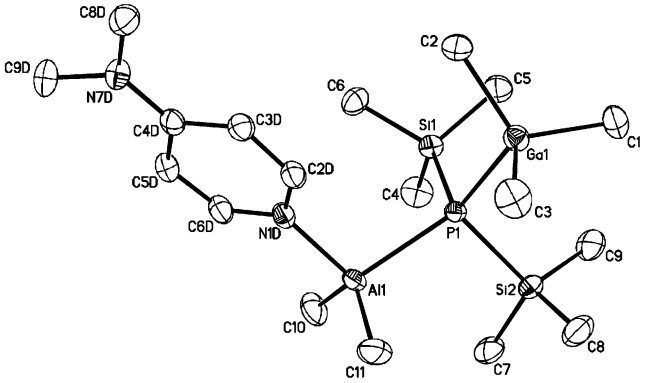

Figure 2. Ortep plot (50% probability ellipsoids) showing the solid-state structure of **2**. Hydrogen atoms are omitted for clarity.

group from Ga to Al to the heterocycle $[Et_2GaP(SiMe_3)_2]_2$ and the mixed-substituted alane adduct dmap−Al(Me)$_2$Et.[9]

On the basis of the NMR investigations a clear trend (Al < Ga < In) of the reactivity of **1**−**3** to undergo the rearrangement reaction is found. While dmap−Al(Me)$_2$P(SiMe$_3$)$_2$−AlMe$_3$ (**1**) is detected in solution (25 °C) even after several days, dmap−Al(Me)$_2$P(SiMe$_3$)$_2$−GaMe$_3$ (**3**) undergoes complete rearrangement to form dmap−AlMe$_3$ and $[Me_2InP(SiMe_3)_2]_2$ within a few minutes even at 0 °C. The observed trend correlates well with the decreasing M−Me bond energies (Al, 84.6 kcal mol^{-1}; Ga, 76.7 kcal mol^{-1}; In, 65.1 kcal mol^{-1}).[10] Several attempts to obtain single crystals of **1**−**3** suitable for an X-ray analysis failed, due to the poor solubility of the adducts at low temperatures and their instability at higher temperatures toward the formation of dmap−AlMe$_3$ and the heterocycles $[Me_2MP(SiMe_3)_2]_2$. Only single crystals of **2** were obtained from a solution in pentane/Et$_2$O. Figure 2 shows its solid-state structure.

As seen in Figure 3, the adduct **2** is cocrystallized with 0.5 equiv of the heterocycle $[Me_2GaP(SiMe_3)_2]_2$ in the asymmetric unit. Obviously, the crystallization conditions again led to a partial decomposition of **2**. In the following, only the structural parameters of the new compound **2** will be discussed.[11] The Al−N (1.974(2) Å) and Al−C bond lengths (average 1.964 Å) of **2** are almost unchanged compared to those of the uncomplexed monomer dmap−Al(Me)$_2$P(SiMe$_3$)$_2$ (Al−N 1.977(2) Å; average Al−C 1.974),[3c] whereas the Al−P bond distance (2.416(1) Å for **2** vs. 2.374(1) Å) is slightly longer, most likely due to the increase in the coordination number of the P atom from 3 to 4. Comparable Al−P distances were observed for $[H_2AlP(SiMe_3)_2]_3$ (average 2.400 Å)[12] and [*i*-BuAlPSiPh$_3$]$_4$ (average 2.415 Å),[13] whereas those found for $[Me_2AlP(SiMe_3)_2]_2$ (average 2.455 Å),[14] $[Et_2AlP(SiMe_3)_2]_2$ (average 2.457 Å),[15] and $[i\text{-}Bu_2AlP(SiMe_3)_2]_2$ (average 2.483 Å)[16] are slightly longer. Despite the increased steric interactions and the increase of the coordination number, the P−Si distances observed for **2** (average 2.254 Å) are surprisingly shorter compared to those of the uncomplexed monomer (average 2.290 Å). The dative Ga−P bond length (2.510(1) Å) is in the lower range of the typical dative Ga−P distances observed for R$_3$Ga−PR′$_3$ adducts with alkyl or silyl substituents (2.45−2.65 Å).[17] Only Me$_3$Ga−PMe$_3$ features a shorter Ga−P bond length of 2.446 Å.[18] The bonding parameters found for the GaMe$_3$ fragment (average M−C 2.00 Å, average C−M−C 113.1°) are within the usual ranges for such Lewis acid−base adducts. Similarly to analogous transition-metal complexes of the type dmap−M(Me)$_2$P(SiMe$_3$)$_2$−M′(CO)$_n$ (M = Al, Ga; M′ = Cr, Fe, Ni)[5] as well as to simple group 13/15 Lewis acid−base adducts R$_3$M−PR′$_3$[19] the pyra-

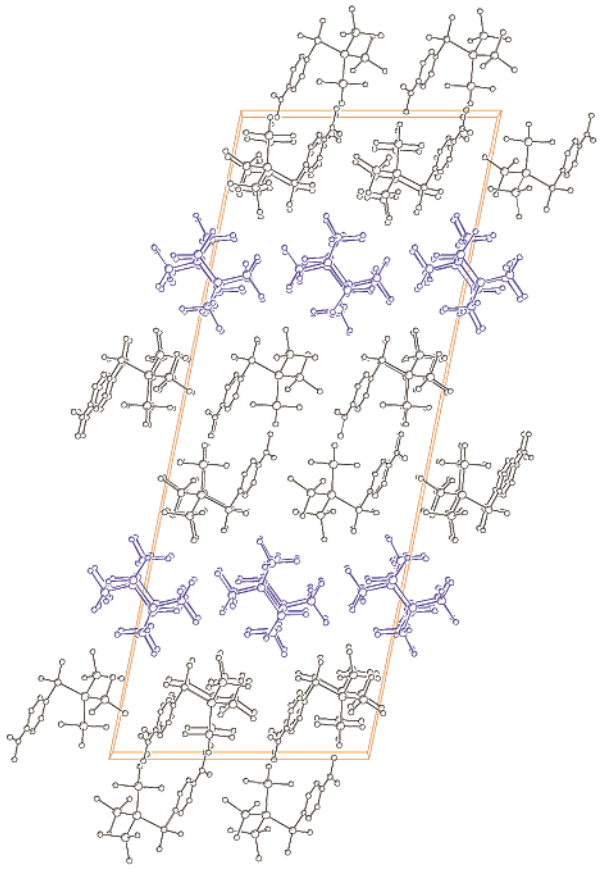

Figure 3. Packing plot (stick-and-ball model) showing the unit cell of **2** containing **2** (black) and $[Me_2GaP(SiMe_3)_2]_2$ (blue). Hydrogen atoms are omitted for clarity.

(9) dmap−Al(Me)$_2$Et can be isolated as rapidly melting crystals that have been identified by ^{1}H and ^{13}C NMR spectroscopy. In solution dismutation to a mixture of dmap−AlMe$_3$, dmap−Al(Me)$_2$Et, dmap−Al(Me)Et$_2$, and dmap−AlEt$_3$ takes place, resulting in a complex NMR signal pattern. Thomas, F.; Schulz, S. Unpublished results.

(10) Allendorf, M. D.; Melius, C. F.; Bauschlicher, C. W. *J. Phys. IV* **1999**, *9*, 23.

(11) The structural parameters of the heterocycle are unchanged compared to those of previously reported structures: (a) Wiedmann, D.; Hausen, H.-D.; Weidlein, J. *Z. Anorg. Allg. Chem*. **1995**, *621*, 1351. (b) Dillingham, M. D. B.; Burns, J. A.; Byers-Hill, J.; Gripper, K. D.; Pennington, W. T.; Robinson, G. H. *Inorg. Chim. Acta* **1994**, *216*, 267.

(12) Janik, J. F.; Wells, R. L.; White, P. S. *Inorg. Chem*. **1998**, *37*, 3561.

(13) Cowley, A. H.; Jones, R. A.; Mardones, M. A.; Atwood, J. L.; Bott, S. G. *Angew. Chem., Int. Ed. Engl*. **1990**, *29*, 1409.

(14) Hey-Hawkins, E.; Lappert, M. F.; Atwood, J. L.; Bott, S. G. *J. Chem. Soc,. Dalton Trans*. **1991**, 939.

(15) Wells, R. L.; McPhail, A. T.; Self, M. F.; Laske, J. A. *Organometallics* **1993**, *12*, 3333.

(16) Krannich, L. K.; Watkins, C. L.; Schauer, S. J.; Lake, C. H. *Organometallics* **1996**, *15*, 3980.

(17) Cambridge Structural Database (CSD) v5.24 (November 2002). Halogen- or hydrogen-substituted adducts X$_3$Ga−PR$_3$ feature shorter bond lengths between 2.35 and 2.46 Å.

(18) Burns, J. A.; Pennington, W. T.; Robinson, G. H. *Organometallics* **1995**, *14*, 1533.

(19) See for instance: Kuczkowski, A.; Schulz, S.; Nieger, M.; Schreiner, P. R. *Organometallics* **2002**, *21*, 1408.

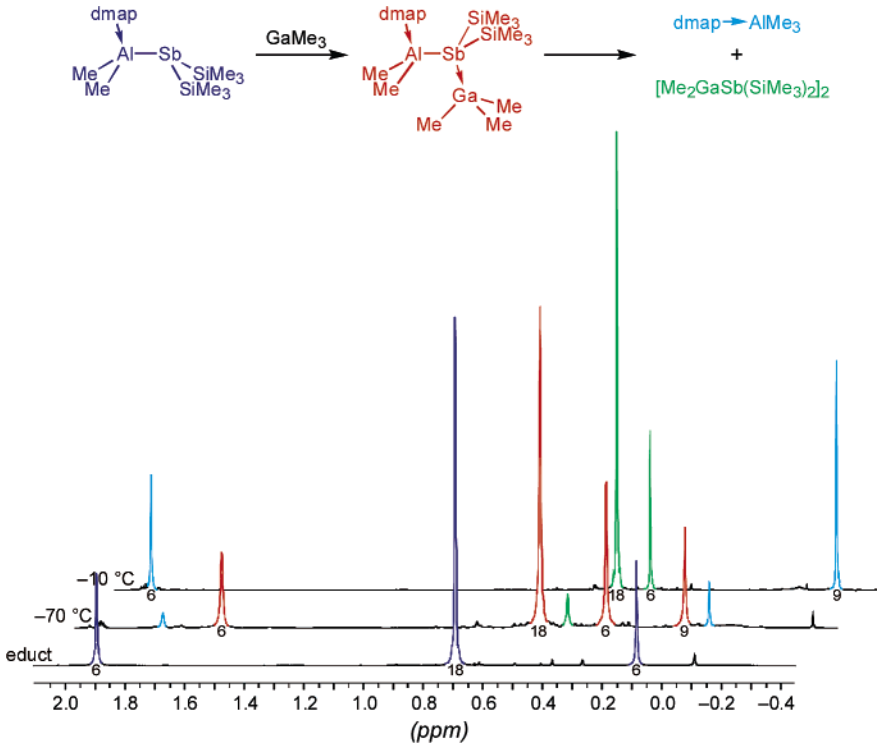

Figure 4. Temperature-dependent ^{1}H NMR spectra of **4** in toluene-d_8 between −70 and +30 °C.

midalization of the P center in **2** decreases upon coordination to the Lewis acid $GaMe_3$. The increase of the sum of the bond angles (Si−P−Si and Al−P−Si angles) of almost 10° (309.8° in the uncomplexed monomer vs. 319.0° in **2**) is comparable to the increase observed for dmap−Al(Me)$_2$P(SiMe$_3$)$_2$−Ni(CO)$_3$ (321.1°).

In an attempt to obtain more stable adducts of the desired type, we performed reactions with the sterically demanding trialkyls *t*-Bu$_3$M (M = Al, Ga), which were previously shown to give stable adducts with a variety of group 15 compounds (eq 2).[3b,20] However, all reactions

$$\text{dmap}-\text{Al(Me)}_2\text{P(SiMe}_3)_2 + \text{M}(t\text{-Bu})_3 \xrightarrow[\text{M = Al, Ga}]{} \text{dmap}-\text{M}(t\text{-Bu})_3 + {}^1/_2[\text{Me}_2\text{AlP(SiMe}_3)_2]_2 \quad (2)$$

with the phosphinoalane dmap−Al(Me)$_2$P(SiMe$_3$)$_2$ only yielded dmap−M(*t*-Bu)$_3$[21] and the heterocycle [Me$_2$AlP(SiMe$_3$)$_2$]$_2$.[8]

In contrast to the observations made for the MMe$_3$ reactions, no *t*-Bu transfer reaction under Al−P bond cleavage takes place. The reactions proceed very slowly at room temperature over the course of several hours, as was shown by ^{31}P and ^{1}H NMR spectroscopy studies. The spectra did not feature signals due to the expected adducts dmap−Al(Me)$_2$P(SiMe$_3$)$_2$−M(*t*-Bu)$_3$ at any time. Two possible reasons may account for this unexpected reaction behavior. Either the formation of the adduct dmap−Al(Me)$_2$P(SiMe$_3$)$_2$−M(*t*-Bu)$_3$ is slower than its dissociation to dmap−M(*t*-Bu)$_3$ and [Me$_2$AlP(SiMe$_3$)$_2$]$_2$ or the adduct is never formed and a simple dmap exchange reaction between the [Me$_2$AlP(SiMe$_3$)$_2$] fragment and M(*t*-Bu)$_3$ occurs. The most likely explanation for the nonformation of the expected adducts and the absence of any *t*-Bu transfer reaction is the steric crowding around the phosphorus center (M(*t*-Bu)$_3$, SiMe$_3$ groups), which significantly decreases the stability of the reaction intermediates. To investigate this question, we performed reactions of the trialkyls MMe$_3$ and M(*t*-Bu)$_3$ (M = Al, Ga) with the analogous stibinoalane dmap−Al(Me)$_2$Sb(SiMe$_3$)$_2$, containing a larger group 15 element (r_{cov}: P, 1.10 Å; Sb, 1.41 Å),[22] which should diminish the influence of steric interactions due to the elongation of the Sb−M (M = Al, Ga) and Sb−Si bond distances (eq 3).

$$\text{dmap}-\text{Al(Me)}_2\text{Sb(SiMe}_3)_2 + \text{MMe}_3 \xrightarrow{-70\ ^\circ\text{C}} \text{dmap}-\text{Al(Me)}_2\text{Sb(SiMe}_3)_2-\text{MMe}_3 \xrightarrow[\text{M = Al, Ga, In}]{>-30\ ^\circ\text{C}} \text{dmap}-\text{AlMe}_3 + {}^1/_3[\text{Me}_2\text{MSb(SiMe}_3)_2]_3 \quad (3)$$

At −10 °C equimolar amounts of MMe$_3$ were added to solutions of dmap−Al(Me)$_2$Sb(SiMe$_3$)$_2$ in pentane. Immediately, white solids precipitated, which were isolated by filtration and identified as dmap−AlMe$_3$ by ^{1}H NMR spectroscopy. After evaporation of the solvent only the heterocycles [Me$_2$MSb(SiMe$_3$)$_2$]$_3$ were retrieved from the filtrates. Obviously, the expected adducts dmap−Al(Me)$_2$Sb(SiMe$_3$)$_2$−MMe$_3$ also are susceptible to the aforementioned rearrangement reaction. Temperature-dependent ^{1}H NMR spectra of dmap−Al(Me)$_2$Sb(SiMe$_3$)$_2$−GaMe$_3$ (see Figure 4) generated in situ at −78 °C point to an increased reactivity of the stibinoalane compared to the phosphinoalane. The adduct is immediately formed by coordination of GaMe$_3$ to the

(20) (a) Schulz, S.; Nieger, M. *J. Chem. Soc., Dalton Trans.* **2000**, 639. (b) Kuczkowski, A.; Schulz, S.; Nieger, M. *Eur. J. Inorg. Chem.* **2001**, 2605. (c) Kuczkowski, A.; Schulz, S.; Nieger, M. *Angew. Chem., Int. Ed.* **2001**, *40*, 4222.

(21) dmap−Al(*t*-Bu)$_3$ was unknown and will be discussed elsewhere in more detail (see also ref 8).

(22) Holleman, A. F.; Wiberg, E. *Lehrbuch der Anorganischen Chemie*, 101st ed.; de Gruyter: Berlin, 1995.

antimony center. Starting at −50 °C (compare −10 °C for the phosphinoalane), signals due to dmap−$AlMe_3$ and the heterocycle $[Me_2GaSb(SiMe_3)_2]_3$ appear in the spectra. At temperatures above −30 °C the adduct has completely disappeared. The increased reactivity toward the rearrangement reaction can be explained by the significantly smaller bond energies of the Al−Sb and Ga−Sb bonds in comparison to those of the respective phosphanes.

In contrast, the addition of equimolar amounts of M(*t*-Bu)$_3$ to the stibinoalane dmap−$Al(Me)_2Sb(SiMe_3)_2$ leads to the formation of the stable adducts dmap−$Al(Me)_2Sb(SiMe_3)_2$−M(*t*-Bu)$_3$ (M = Al (**4**), Ga (**5**); eq 4). **4** and **5**

$$\text{dmap}-\text{Al(Me)}_2\text{Sb(SiMe}_3)_2 + \text{M}(t\text{-Bu})_3 \xrightarrow{-20\ ^\circ\text{C}}$$
$$\text{dmap}-\text{Al(Me)}_2\text{Sb(SiMe}_3)_2-\text{M}(t\text{-Bu})_3 \xrightarrow[\text{M = Al}]{\text{room temp, slow}}$$
$$\text{M = Al (4), Ga (5)}$$
$$\text{dmap}-\text{Al}(t\text{-Bu})_3 + {}^1/_3[\text{Me}_2\text{AlSb(SiMe}_3)_2]_3 \quad (4)$$

precipitate in pentane at −20 °C as colorless solids within 5 min and were isolated by filtration. They were characterized by elemental analysis, mass and multinuclear NMR spectroscopy (^{1}H, ^{13}C{^{1}H}), and single-crystal X-ray diffraction.

^{1}H NMR spectra of freshly prepared samples of **4** and **5** show the expected resonances due to the organic ligands. Those of dmap, Me, and $SiMe_3$ in **4** and **5** are slightly shifted upfield compared to dmap−$Al(Me)_2Sb(SiMe_3)_2$, whereas those of M(*t*-Bu)$_3$ are shifted downfield compared to pure M(*t*-Bu)$_3$. Such findings are typical for stibine−alane and −gallane adducts.[20a,23] The NMR spectra of **4** had to be recorded within a short period of time due to its thermal instability in solution. After a few hours at ambient temperature they show additional resonances due to the presence of dmap−Al(*t*-Bu)$_3$ and $[Me_2AlSb(SiMe_3)_2]_3$. This can be explained by ligand exchange reactions, as observed in the reaction of dmap−$Al(Me)_2P(SiMe_3)_2$ and Al(*t*-Bu)$_3$. In contrast, an NMR sample of **5** after heating to 60 °C for several hours features no additional resonances, indicating **5** to be significantly more thermally stable in solution. Mass spectra of both **4** and **5** did not show the molecular ion peaks. Only signals due to the formation of dmap$^+$ (*m*/*z* 122), M(*t*-Bu)$_2^+$ (*m*/*z* 141 (Al), 183 (Ga)), and Sb$(SiMe_3)_3^+$ (*m*/*z* 340) were found, as a result of excessive fragmentation reactions under these conditions.

The solid-state structures of **4** and **5** were determined by X-ray diffraction (Figures 5 and 6). Single crystals were obtained from concentrated toluene solutions at −30 °C. **4** crystallizes in the orthorhombic space group $P2_12_12_1$ (No. 19) with one toluene molecule in the asymmetric unit, and **5** crystallizes in the monoclinic space group *Pn* (No. 7). In **5** the Ga(*t*-Bu)$_3$ fragment is disordered with Ga(*i*-Bu)(*t*-Bu)$_2$, resulting from small impurities in the starting reagent Ga(*t*-Bu)$_3$. The NMR spectrum of a macroscopic sample of **5** shows that the overall content of the Ga(*i*-Bu)(*t*-Bu)$_2$ adduct in the product is below 5%; consequently, it will not be discussed in further detail.

The Al−N (1.968(3) Å, **4**; 1.961(7) Å, **5**) and average Al−C (1.97 Å, **4**; 1.97 Å, **5**) bond distances as well as

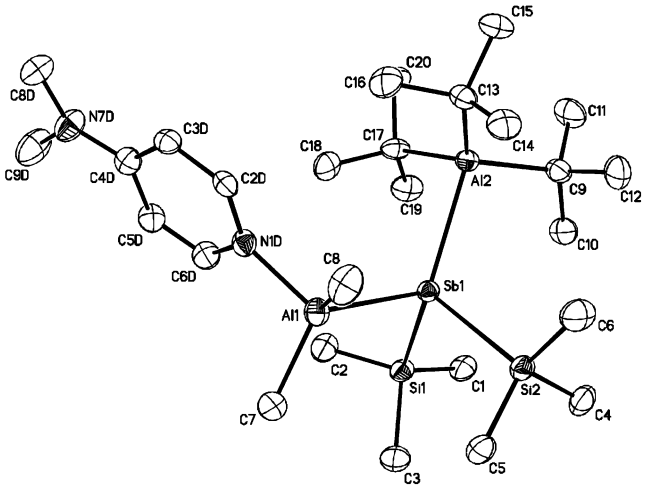

Figure 5. Ortep plot (50% probability ellipsoids) showing the solid-state structure of **4**. Hydrogen atoms are omitted for clarity.

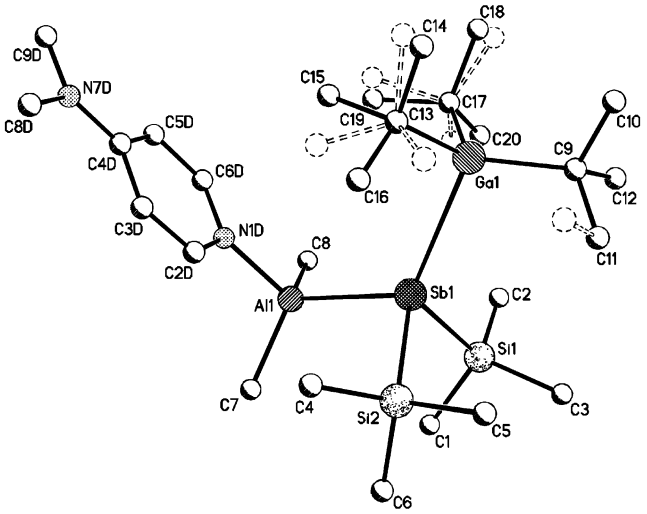

Figure 6. Stick-and-ball plot showing the solid-state structure of **5**. Hydrogen atoms are omitted for clarity. The Ga(*t*-Bu)$_3$ fragment is disordered with Ga(*i*-Bu)(*t*-Bu)$_2$.

the C−Al−C (117.2(2)°, **4**; 115.8(4)°, **5**) and average N−Al−C (105.5°, **4**; 106.5°, **5**) bond angles within the dmap−$Al(Me)_2Sb(SiMe_3)_2$ fragments found in **4** and **5** are almost unchanged compared to the corresponding values observed in dmap−$Al(Me)_2Sb(SiMe_3)_2$ (Al−N, 1.978(1) Å; Al−C, 1.970 Å; C−Al−C, 116.5(1)°; N−Al−N, 105.9°).[4a] In contrast, the average Sb−Si (2.57 Å, **4**; 2.58 Å, **5**) and Al−Sb bond distances (Al1−Sb1: 2.725(1) Å, **4**; 2.726(3) Å, **5**) are slightly elongated (dmap−$Al(Me)_2Sb(SiMe_3)_2$: Sb−Si, 2.548 Å; Al−Sb, 2.691(1) Å), most likely caused by the increase in the coordination number from 3 to 4 (Sb) and the strong repulsive interactions between the $SiMe_3$ groups and the bulky M(*t*-Bu)$_3$ fragment. The Al−Sb σ-bond distances are almost identical with the average distance observed in the heterocycle $[Me_2AlSb(SiMe_3)_2]_3$ (2.72 Å). This is unexpected, since the Al−Sb bonds in the heterocycle are formally mixtures of σ and dative bonds according to their definition as *head-to-tail* adducts. The dative M−Sb bond lengths (2.869(1) Å, **4**; 2.889(1) Å, **5**) are unexpectedly short, despite the very bulky M(*t*-Bu)$_3$ group. For instance, the Ga−Sb bond distance found in *t*-Bu_3Ga−$Sb(SiMe_3)_2$ (3.027(2) Å)[24] is about 14 pm longer

(23) Schulz, S.; Kuczkowski, A.; Nieger, M. *J. Organomet. Chem.* **2000**, *604*, 202.

than that in **5**. These findings point to a high Lewis basicity of the Sb center in **4** and **5**, most likely caused by the presence of the electropositive Al fragment, leading to strong attractive acid−base interactions. This agrees very well with the observations for the transition-metal complexes dmap−$M(Me)_2E(SiMe_3)_2$−$M'(CO)_n$, which demonstrate the coordinative E−M′ interaction to be of almost exclusive σ-donor character, whereas the π-acceptor abilities of the pnicogen centers E are very weak.[5b] The M(*t*-Bu)$_3$ fragments show no surprising structural parameters: the increased average M−C bond lengths (2.03 Å, **4**; 2.03 Å, **5**) and the decreased average C−M−C bond angles (115°, **4**; 114°, **5**) in comparison to free Al(*t*-Bu)$_3$ (2.00 Å, 120°) and Ga(*t*-Bu)$_3$ (2.01 Å, 120°)[25] are in accordance with the model described by Haaland.[26]

The most striking structural features of **4** and **5** are reflected by the geometrical changes of the Sb centers upon adduct formation. To our surprise, the coordination of the Lewis acid M(*t*-Bu)$_3$ *decreases* the degree of pyramidalization of the Sb center in **4** (sum of bond angles Si−E−Si and Si−E−Al: 298.3°) and **5** (298.2°) compared to that of dmap−$Al(Me)_2Sb(SiMe_3)_2$ (302.4°) by almost 4°. This is in sharp contrast to findings observed for **2** as well as for transition-metal complexes.[5b] According to the VSEPR model, assuming an *electron lone pair* to be sterically more demanding than a *donor electron pair*, and a partial rehybridization of the Sb lone pair upon adduct formation (*p*-character increases), the sum of the bond angles in **4** and **5** were expected to increase. These findings are attributed to the steric interactions between the extremely bulky M(*t*-Bu)$_3$ group and the organic ligands bound to the Sb center ($SiMe_3$ groups), which are enhanced by the short dative M−Sb bond. A comparison of **4** and **5** with the Ni complex dmap−$Al(Me)_2Sb(SiMe_3)_2$−$Ni(CO)_3$, containing the sterically less demanding Ni(CO)$_3$ fragment, clearly reveals the influence of such repulsive interactions on the geometry of the Sb center, whose absence leads to a significantly increased sum of bond angles around the Sb center (314.3°).[5a] The role of repulsive interactions has also been previously observed for transition-metal complexes. The sum of bond angles of the P center in the phosphinoalane complexes dmap−$Al(Me)_2P(SiMe_3)_2$−$M(CO)_n$ ($M(CO)_n$ = Ni(CO)$_3$, Fe(CO)$_4$, Cr(CO)$_5$) steadily decreases with increasing steric demand of the metal fragment (Ni(CO)$_3$, 321.1°; Fe(CO)$_4$, 318.9°; Cr(CO)$_5$, 313.4°). However, in contrast to **4** and **5**, even the Cr(CO)$_5$ complex features a slightly increased sum of bond angles compared to the uncomplexed monomer.

Conclusions

The reactivity of phosphino- and stibinoalanes dmap−$Al(Me)_2E(SiMe_3)_2$ (E = P, Sb) toward group 13 trialkyls has been studied in detail. The desired compounds dmap−$Al(Me)_2E(SiMe_3)_2$−MR_3 can be synthesized; however, their stability in solution strongly depends on the group 13 trialkyl and the pnicogen center. Adducts of the sterically less demanding trialkyls MMe_3 readily undergo rearrangement reactions, leading to the formation of the heterocycles $[Me_2ME(SiMe_3)_2]_x$ (M = Al, Ga, In; E = P, Sb). The tendency toward this rearrangement reaction was shown to increase with increasing the atomic number of both the pnicogen center and the group 13 atom of the group 13 trialkyl MMe_3. Steric interactions play a limiting role in the stability of the as-mentioned adducts. Consequently, only the stibinoalane dmap−$Al(Me)_2Sb(SiMe_3)_2$, containing the larger Sb atom, forms stable adducts with the sterically more demanding trialkyls M(*t*-Bu)$_3$. In contrast, reactions of dmap−$Al(Me)_2P(SiMe_3)_2$ with M(*t*-Bu)$_3$ occur under abstraction of dmap from the phosphinoalane and the formation of dmap−M(*t*-Bu)$_3$. Single-crystal X-ray studies clearly revealed the strong σ-donor character of the monomeric compounds, leading to short E−M (M = Al, Ga) dative bond distances. The utility of the reported reaction pathway for the general synthesis of compounds of the desired type and a possible transfer to other metal alkyls is currently under investigation.

Experimental Section

General Information. All manipulations were performed in a glovebox under an Ar atmosphere or with standard Schlenk techniques. Solvents were dried over sodium/potassium alloy and degassed prior to use. $AlMe_3$ was obtained from ABCR and used as received. dmap−$Al(Me)_2P(SiMe_3)_2$,[3c] dmap−$Al(Me)_2Sb(SiMe_3)_2$,[3a] Al(*t*-Bu$_3$),[27] Ga(*t*-Bu$_3$),[28] $GaMe_3$,[29] and $InMe_3$[30] were prepared according to literature methods. ^{1}H and ^{13}C{^{1}H} NMR spectra were recorded using a Bruker DPX300 NMR spectrometer and are referenced to the resonances of the solvents (benzene-d_6, δ(^{1}H) 7.15, δ(^{13}C) 128.0; toluene-d_8, δ(^{1}H) 2.03, δ(^{13}C) 20.4). ^{31}P{^{1}H} spectra are referenced to external H_3PO_4 (δ(^{31}P) 0). Mass spectra (EI) were recorded on a VG Masslab 12-250 spectrometer. Melting points were measured in sealed capillaries and were not corrected. Elemental analyses of **4** and **5** were performed at the Mikroanalytisches Labor der Universität Bonn. Several attempts to obtain reliable elemental analyses of **1**−**3** failed due to their poor thermal stability.

General Preparation of dmap−$Al(Me)_2P(SiMe_3)_2$−MMe_3 (M = Al (1), Ga (2), In (3)). MMe_3 (1.0 mmol: Al, 0.07 g; Ga, 0.11 g; In, 0.16 g) was added to a solution of dmap−$Al(Me)_2P(SiMe_3)_2$ (1.0 mmol, 0.36 g) in 10 mL of pentane/Et_2O (10:1) at −30 °C, immediately yielding a white suspension. **1**−**3** were isolated by filtration as colorless solids. Recrystallization from pentane/Et_2O (1:1) yielded colorless crystals of **2** suitable for X-ray structure analysis.

1: yield 91%; $C_{18}H_{43}Al_2N_2PSi_2$ (M_r = 428.66); ^{1}H NMR (300 MHz, toluene-d_8, −10 °C) δ −0.28 (d, $^3J_{PH}$ = 4.1 Hz, 9H, $AlMe_3$), −0.12 (d, $^3J_{PH}$ = 2.3 Hz, 6H, $AlMe_2$), 0.42 (d, $^3J_{PH}$ = 4.3 Hz, 18H, $SiMe_3$), 1.82 (s, 6H, NMe_2), 5.62 (dd, $^3J_{HH}$ = 6.0 Hz, $^4J_{HH}$ = 1.3 Hz, 2H, C3−H), 7.97 (dd, $^3J_{HH}$ = 6.0 Hz, $^4J_{HH}$ = 1.3 Hz, 2H, C2−H); ^{13}C NMR (75 MHz, toluene-d_8, −30 °C) δ −7.1 ($AlMe_3$), −3.7 (d, $^2J_{PC}$ = 12.3 Hz, $AlMe_2$), 3.6 (d, $^2J_{PC}$ = 7.4 Hz, $SiMe_3$), 37.8 (NMe_2), 106.2 (C3), 146. 3 (C2), 154.4 (C4); ^{31}P NMR (121.5 MHz, toluene-d_8, −10 °C) δ −262.0; MS (12 eV, 75 °C) *m*/*z* (%) 250 ($P(SiMe_3)_3^+$, 4), 179 (dmap−$AlMe_2^+$, 16), 178 ($HP(SiMe_3)_2^+$, 9), 122 (dmap$^+$, 100), 73 (Me_3Si^+, 4), 57 (Me_2Al^+, 13); mp 70−100 °C dec.

2: yield 82%; $C_{18}H_{43}AlGaN_2PSi_2$ (M_r = 471.40); ^{1}H NMR (300 MHz, toluene-d_8, −10 °C) δ −0.10 (d, $^3J_{PH}$ = 2.2 Hz, 6H,

(24) Wells, R. L.; Foos, E. E.; White, P. S.; Rheingold, A. L.; Liable-Sands, L. M. *Organometallics* **1997**, *16*, 4771.
(25) Rankin, D. W. H.; Barron, A. R. Personal communication.
(26) Haaland, A. In *Coordination Chemistry of Aluminum*; Robinson, G. H., Ed.; VCH: Weinheim, Germany, 1993.
(27) Lehmkuhl, H.; Olbrysch, O.; Nehl, H. *Liebigs Ann. Chem.* **1973**, 708.
(28) Kovar, R. A.; Derr, H.; Brandau, D.; Callaway, J. O. *Inorg. Chem.* **1975**, *14*, 2809.
(29) Foster, D. F.; Cole-Hamilton, D. J.; Jones, R. A. *Inorg. Synth.* **1997**, *31*, 46.
(30) Reier, F. W.; Wolfram, P.; Schumann, H. *J. Cryst. Growth* **1988**, *93*, 41.

Table 1. Crystallographic Data and Measurements for 2, 4, and 5

	2	4	5
mol formula	$C_{18}H_{43}N_2AlSi_2PGa \cdot {}^1/_2C_{16}H_{48}Si_4P_2Ga_2$	$C_{27}H_{61}Al_2N_2SbSi_2 \cdot$(toluene)	$C_{27}H_{61}AlGaN_2SbSi_2$
fw	1497.07	737.80	688.41
cryst syst	monoclinic	orthorhombic	monoclinic
space group	*C*2/*c* (No. 15)	$P2_12_12_1$ (No. 19)	*Pn* (No. 7)
a, Å	48.0704(4)	9.7892(1)	11.1340(3)
b, Å	9.4362(1)	15.4362(2)	14.2679(4)
c, Å	18.8928(20)	28.0419(4)	11.5519(3)
β, deg	101.530(1)	90	93.612(2)
V, Å^3	8396.87(14)	4237.36(9)	1831.48(9)
Z	4	4	2
radiation (wavelength, Å)	Mo Kα (0.710 73)	Mo Kα (0.710 73)	Mo Kα (0.710 73)
μ, mm^{-1}	1.512	0.771	1.579
T, K	123(2)	123(2)	123(2)
D_{calcd}, g cm^{-3}	1.184	1.157	1.248
cryst dimens (mm^3)	0.40 × 0.20 × 0.10	0.40 × 0.15 × 0.10	0.25 × 0.15 × 0.21
$2\theta_{max}$, deg	55.0	50.0	50.0
no. of rflns recorded	57 807	35 830	23 248
no. of nonequiv rflns recorded	9565	7470	5995
R_{merge}	0.0546	0.0630	0.0598
no. of params refined/restraints	336/0	373/0	286/467
R1;[a] wR2[b]	0.0264, 0.0685	0.0273, 0.0536	0.0443, 0.1134
goodness of fit[c]	0.971	0.983	1.059
final max, min $\Delta\rho$, e Å^{-3}	0.674, −0.533	0.551, −0.559	1.163, −0.951

[a] $R1 = \sum(||F_o| - |F_c||)/\sum|F_o|$ (for $I > 2\sigma(I)$). [b] $wR2 = \{\sum[w(F_o^2 - F_c^2)^2]/\sum[w(F_o^2)^2]\}^{1/2}$ (for all data). [c] Goodness of fit $= \{\sum[w(|F_o^2| - |F_c^2|)^2]/(N_{observns} - N_{params})\}^{1/2}$.

Table 2. Selected Bond Lengths (Å) and Angles (deg) of 2, 4, and 5

	2	4	5
Al(1)−N(1d)	1.974(2)	1.968(3)	1.961(7)
Al(1)−C[a]	1.96	1.97	1.97
Al(1)−E(1)	2.416(1)	2.725(1)	2.726(3)
E(1)−Si[a]	2.25	2.57	2.58
E(1)−M	2.510(1)	2.869(1)	2.889(1)
M−C[a]	2.00	2.03	2.03
C−Al(1)−C	118.9(2)	117.2(2)	115.8(4)
Al(1)−E(1)−Si(1)	107.6(1)	102.8(1)	96.4(1)
Al(1)−E(1)−Si(2)	103.8(1)	98.0(1)	102.7(1)
Si(1)−E(1)−Si(2)	107.5(1)	97.5(1)	99.2(1)
C−M−C[a]	113.1	115.0	114.0
N−Al−E−M	54.5(1)	38.9(1)	−43.8(2)

[a] Average values.

$AlMe_2$), 0.08 (s, 9H, $GaMe_3$), 0.44 (d, $^3J_{PH}$ = 4.2 Hz, 18H, $SiMe_3$), 1.78 (s, 6H, NMe_2), 5.59 (dd, $^3J_{HH}$ = 6.0 Hz, $^4J_{HH}$ = 1.3 Hz, 2H, C3−H), 8.01 (dd, $^3J_{HH}$ = 6.0 Hz, $^4J_{HH}$ = 1.3 Hz, 2H, C2−H); ^{13}C NMR (75 MHz, toluene-d_8, −10 °C) δ −0.9 (br, $AlMe_2$), 1.6 ($GaMe_3$), 4.1 (d, $^2J_{PC}$ = 7.4 Hz, $SiMe_3$), 38.3 (NMe_2), 106.7 (C3), 146.6 (C2), 155.6 (C4); ^{31}P NMR (121.5 MHz, toluene-d_8, −10 °C) δ −262.4; mp 90−120 °C dec.

3: yield 86%; $C_{18}H_{43}AlInN_2PSi_2$ (M_r = 516.50); ^{31}P NMR (121.5 MHz, toluene-d_8, −30 °C) δ −278.0; MS (12 eV, 50 °C) *m*/*z* (%) 307, ($Me_2AlPTms_3$, 4), 250 ($P(SiMe_3)_3$, 5), 235 ($(Me_3Si)_2PSiMe_2^+$, 3), 179 (dmap−$AlMe_2^+$, 34), 145 (Me_2In^+, 12) 122 (dmap$^+$, 100), 73 (Me_3Si^+, 8), 57 (Me_2Al^+, 50); mp 85−120 °C dec.

General Preparation of dmap−Al(Me)$_2$Sb(SiMe$_3$)$_2$−M(*t*-Bu)$_3$ (M = Al (4), Ga (5)). *t*-Bu_3M (1.0 mmol: Al, 0.20 g; Ga, 0.24 g) was added slowly to a solution of dmap−$Al(Me)_2Sb(SiMe_3)_2$ (1.0 mmol, 0.45 g) in 10 mL of pentane at ambient temperature. Within 5 min, dmap−$Al(Me)_2Sb(SiMe_3)_2$−M(*t*-$Bu)_3$ (M = Al (**4**), Ga (**5**)) precipitate as white solids, which were isolated by filtration. Recrystallization from toluene yielded colorless crystals suitable for X-ray structure analysis.

4: yield 73%; ^{1}H NMR (300 MHz, toluene-d_8, −20 °C) δ 0.04 (s, 6H, $AlMe_2$), 0.67 (s, 18H, $SiMe_3$), 1.33 (s, 27H, *t*-Bu), 1.77 (s, 6H, NMe_2), 5.47 (d, $^3J_{HH}$ = 7.2 Hz, 2H, C3−H), 7.82 (d, $^3J_{HH}$ = 7.4 Hz, 2H, C2−H); ^{13}C NMR (75 MHz, toluene-d_8, −20 °C) δ −4.0 (br, $AlMe_2$), 5.9 ($SiMe_3$), 19.2 (CMe_3), 33.7 (CMe_3), 38.2 (NMe_2), 106.4 (C3), 146.4 (C2), 155.2 (C4); MS (12 eV, 75 °C) *m*/*z* (%) 57 (85) *t*-Bu^+, 73 (50) $SiMe_3^+$, 122 (100) DMAP$^+$, 141 (70) *t*-Bu_2Al^+, 198 (10) *t*-Bu_3Al^+, 252 (70) $Me_2AlSbSiMe_3^+$, 340 (95) $Sb(SiMe_3)_3^+$, 488 (20) $Me_3Al_2Sb_2(SiMe_3)_2^+$, 536 (1) $Sb_2(SiMe_3)_4^+$; mp 103−105 °C dec. Anal. Calcd (found) for $C_{27}H_{61}Al_2N_2SbSi_2$ (M_r = 645.68): C, 50.2 (49.8); H, 9.5 (9.1).

5: yield 88%; ^{1}H NMR (300 MHz, C_6D_6, 30 °C) δ 0.05 (s, 6H, $AlMe_2$), 0.69 (s, 18H, $SiMe_3$), 1.40 (s, 27H, *t*-Bu), 1.89 (s, 6H, NMe_2), 5.65 (d, $^3J_{HH}$ = 7.2 Hz, 2H, C3−H), 7.95 (d, $^3J_{HH}$ = 7.4 Hz, 2H, C2−H); ^{13}C NMR (75 MHz, C_6D_6, 30 °C) δ −4.0 (br, $AlMe_2$), 6.2 ($SiMe_3$), 26.8 (CMe_3), 33.8 (CMe_3), 38.2 (NMe_2), 106.6 (C3), 146.7 (C2), 155.4 (C4); MS (12 eV, 50 °C) *m*/*z* (%) 56 (5) *t*-Bu^+, 73 (15) $SiMe_3^+$, 122 (60) DMAP$^+$, 183 (100) *t*-Bu_2Ga^+, 252 (20) $Me_2AlSbSiMe_3^+$, 340 (15) $Sb(SiMe_3)_3^+$, 488 (5) $Me_3Al_2Sb_2(SiMe_3)_2^+$; mp 134−137 °C dec. Anal. Calcd (found) for $C_{27}H_{61}AlGaN_2SbSi_2$ (M_r = 688.41): C, 47.1 (47.3); H, 8.9 (8.8).

X-ray Structure Solution and Refinement. Crystallographic data of **2**, **4**, and **5** are summarized in Table 1 and selected bond lengths and angles in Table 2. Figures 2, 5, and 6 show diagrams of the solid-state structures of **2**, **4**, and **5**. Data were collected on a Nonius Kappa-CCD diffractometer. The structures were solved by direct methods (SHELXS-97)[31] and refined by full-matrix least squares on F^2. Empirical absorption corrections were applied. All non-hydrogen atoms were refined anisotropically and hydrogen atoms by a riding model (SHELXL-97).[32] The absolute structure of **4** was determined by refinement of Flack's *x* parameter (x = 0.00(2)).[33] **5** is a racemic twin (x = 0.38(3)), and the Ga(*t*-Bu)$_3$ fragment is disordered with Ga(*i*-Bu)(*t*-$Bu)_2$.

Acknowledgment. S.S. gratefully acknowledges financial support by the Deutsche Forschungsgemeinschaft (DFG), the Fonds der Chemischen Industrie (FCI), the Bundesministerium für Bildung, Wissenschaft, Forschung und Technologie (BMBF) and Prof. E. Niecke, Universität Bonn. F.T. is grateful to the Fonds der Chemischen Industrie for a fellowship award.

Supporting Information Available: Tables of bond distances, bond angles, anisotropic temperature factor parameters, and fractional coordinates for **2**, **4**, and **5**. This material is available free of charge via the Internet at http://pubs.acs.org.

OM0303451

(31) Sheldrick, G. M. SHELXS-97, Program for Structure Solution. *Acta Crystallogr., Sect. A* **1990**, *46*, 467.
(32) Sheldrick, G. M. SHELXL-97, Program for Crystal Structure Refinement; Universität Göttingen, Göttingen, Germany, 1997.
(33) Flack, H. P. *Acta Crystallogr., Sect. A* **1983**, *39*, 876.